MAP-BASED HEIGHT ABOVE GROUND ESTIMATION FOR SAFE OPERATION MONITORING OF UNMANNED AIRCRAFT IN VERY LOW LEVEL AIRSPACES

S. Schopferer*, S. Schirmer*, F. Jünger*, H. Loheide*
* DLR Institute of Flight Systems, Braunschweig, Germany

Abstract

According to current European regulations, most common drone operations are limited to a maximum altitude of 120 m above ground. However, a direct measurement of the height above ground is usually not available for small drones. Consequently, ensuring compliance to height above ground constraints may prove to be difficult for many scenarios, especially when flying over complex terrain or beyond the visual line-of-sight of a remote pilot. In this work, we investigate the use of a satellite-based navigation and digital terrain maps to estimate the height above ground. We propose to integrate this estimation into a runtime assurance architecture with a safe operation monitor ensuring compliance to the maximum height above ground imposed by regulatory or operational constraints. We assess the feasibility and limitations of the approach, by analyzing sources of errors including navigation uncertainty and elevation data accuracy. We present the design and implementation details of a height above ground estimation and monitoring system and show results from flight tests with a multicopter drone. The presented results indicate the practicability and current limitations of a map-based height above ground estimation for drones operated in very low level airspaces.

Keywords

UAS; very low level operations; height above ground estimation; digital elevation model; safe operation monitoring

1. INTRODUCTION

According to current European regulations, most types of drone operations are limited to a maximum altitude of 120 m above ground [1]. However, most common drones rely solely on Global Navigation Satellite Systems (GNSS) for navigation. A direct measurement of the height above ground (HAG) is usually not available in these systems. For operations within visual line of sight, the HAG can be either visually estimated by a pilot on the ground or assessed by comparing GNSS altitude before and after take-off, e.g. from telemetry data at the ground control station. However, for more challenging scenarios, it may prove difficult to obtain the current HAG, for example when flying over uneven or hilly terrain, when operating beyond visual line of sight, or in the case of autonomous flight where a visual judgement of a pilot on the ground is not available. Consequently, ensuring compliance with HAG constraints may prove to be difficult for many scenarios. Therefore, we propose the use of digital elevation models (DEMs) for unmanned aircraft, which can be used to estimate the HAG by comparing the GNSS altitude readings with the local map terrain elevation information. This approach is consistent with manned aviation, which already uses such maps for terrain awareness and warning systems (TAWS).

In this work, we investigate the integration of a GNSS- and map-based HAG estimation for an onboard Safe Operation Monitor for unmanned aircraft. By monitoring the minimum and maximum HAG limits, the system improves the situational awareness and – in case of autonomous flight – increases the onboard situational intelligence required to maintain the safety of the operation. We assess the feasibility and limitations of the approach, by analyzing sources of errors including GNSS uncertainty, projection and transformation errors and DEM accuracy. Furthermore, we discuss the definitions of very low level (VLL) airspaces and HAG constraints provided by current EU drone regulations. We present the design and implementation details of a HAG estimator and show results from flight tests with a multicopter drone running the HAG estimator on its onboard computer. The presented results indicate the practicability and limitations of a HAG estimation for safe operation monitoring of drones in VLL airspaces.

2. RELATED WORK

The problem of height estimation for drones has been discussed in literature and media. As described in [2], the drone operator community has recognized the problem of acquiring the correct HAG for VLL operations and the need to differentiate between the height

doi: 10.25967/610406

reported by the drone after take-off, the actual HAG, and altitude above mean sea level as used by manned aviation as a primary vertical reference.
In [3], a study regarding the capability of drone pilots to estimate their drone's height is presented with the conclusion that pilots are "poor at judging the altitude of their ownship". Hence, even for operations within visual line of sight, the use of a HAG indication is advisable. In [4], the height estimation accuracy of an off-the-shelf multicopter drone is assessed in the context of remote sensing applications. Both GNSS-based and barometric altitude measurements were used. While height estimates proved to be more accurate when the drone was reset in between measurements, the measurements in continuous flight showed errors in the range of a few meters.
Both, GNSS-based and barometric HAG estimation, require a reference measurement to compare to. In locally constrained operations above even terrain, the estimation can be initialized on the ground, however, when over-flying uneven terrain this poses a problem. Other approaches to directly measure the HAG have been discussed in the literature. In [5], a small-scale pulse correlation radar device is evaluated and compared to an off-the-shelf LiDAR sensor to directly measure the HAG. The radar-based approach is found to be more robust in detecting the ground below sparse vegetation. While the LiDAR sensor was limited to a range of approximately 15 m, the range of the radar device can be scaled up to 80 m, hence, providing sufficient range to safe-guard many VLL operations. In [6], a monocular vision-based approach is described using only a single downward-looking camera and exploiting optical flow of features detected in the camera images. The results indicate that the relative error of the monocular height estimation stays within 20 % relative error. A similar approach is described in [7]. The authors point out the general challenge of implementing a vision-based estimation that performs well over a broad range of altitudes and environments. While radar- or vision-based methods provide a direct measurement of HAG, thus solving the problem of over-flying uneven terrain, these methods require sensors that are not commonly part of navigation systems of small drones.
In manned aviation, radio altimetry, i.e. the use of radar sensors to measure altitude above-ground-level (AGL), has been a key measure to prevent controlled flight into terrain for decades. The avionics systems that integrate the automated terrain warning and avoidance capabilities are named Ground Proximity Warning System (GPWS) or Terrain Awareness and Warning System (TAWS) and similar. Besides the radar sensor, DEMs are used by these technologies to predict the evolution of the aircraft's altitude above ground on the current flight track and to issue warnings before entering safety-critical situations [8]. The US Air Force, NASA, and Lockheed Martin have developed and deployed the Automatic Ground Collision Avoidance System (Auto-GCAS) on the Air Force's F-16 and F-35 fleets. This system uses a DEM of the terrain in its terrain sensing and collision prediction algorithm. Of particular interest to this paper is the work of those NASA researchers in the development of the Dryden Remotely Operated Integrated Drone (DROID) Small-UAV Auto-GCAS, a small (less than 55 lbs or 25 kg) unmanned aircraft equipped with a Piccolo autopilot where the Auto-GCAS software was integrated into an Android smartphone [9]. The work on Small-UAV Auto-GCAS shows how DEMs can be useful in estimating HAG, but the focus lies in the use of this data for a ground collision prediction and avoidance system. Whereas this work focuses on the use of HAG estimation using DEMs to maintain compliance to regulatory requirements of altitude above ground for operation of small unmanned aircraft. The authors also believe that this work can provide more benefit for small UAS that are intended to operate continuously within a certain band of altitude or HAG, such as for aerial surveying or agricultural missions.

3. ANALYSIS OF GNSS- AND MAP-BASED HAG

The concept of GNSS- and map-based HAG estimation is simple: the current HAG value is the difference between the current position provided by a GNSS and the terrain elevation obtained by querying the map. Unfortunately, there are many technical details that must be considered before implementing such a concept. For instance, the GNSS comes with inaccuracies of its readings and the map provides only a limited spatial resolution. Moreover, there are even different definitions of HAG.
In the following, we address such important details regarding the map-based HAG estimation to further refine and also validate the concept. First, we compare various definitions of the HAG that are found in the research literature and legal documents. Then, we discuss the availability and accuracy of DEMs and give a qualitative error analysis accounting for the limited accuracy of GNSS measurements and elevation data.

3.1. Height Above Ground Definitions and Limitations

The main goal to impose an upper HAG limit for drone operation is to establish a separation between unmanned and manned air traffic. The Standardized European Rules of the Air state that aircraft flown under visual flight rules (VFR) are to maintain heights of "150 m (500 ft) above the ground or water, or 150 m (500 ft) above the highest obstacle within a radius of 150 m (500 ft) from the aircraft" [10, sect. IV / p.57ff.]. Exceptions to this rule exist for special type of aircraft such as gliders and of course for take-off and landings. More conservative, i.e. higher HAG limits for manned aviation exist for flight over congested areas or flight under instrument flight rules (IFR).
The definition of the HAG lower limit for manned aviation can be interpreted in a geometric way as a cylindrical constraint where the axis of the cylinder is vertical and the radius of the cylinder is 150 m. The minimum

altitude above uneven terrain can be obtained by shifting the cylinder upwards from the ground until terrain and obstacles are beneath its lower surface. The upper surface of the cylinder corresponds to the HAG lower limit.

As stated in [1], “in general, manned aircraft do not use very low level (VLL) airspace, as it is below the minimum safe height to perform an emergency procedure”. This is the reasoning leading to the limitation of drone operations to a maximum HAG. Consequently, the 150 m (500 ft) limit, which serves as the lowest possible HAG limit for manned aircraft, is used as a reference to establish an air risk buffer of 100 ft between manned and unmanned air traffic leading to the upper HAG limit of 120 m for drones. However, the exact definition of this upper limit is different to the cylindrical constraint defined for manned aircraft.

For operations in the EASA open category, the remote pilot must keep the UA “at a distance less than 120 m (400 ft) from the terrain” such that “the maximum height that the UA may reach changes according to the topography of the terrain” [1, p. 249]. For operations in the EASA specific category, which encompasses more complex operational scenarios, no general HAG limit is specified. However, the intrinsic air risk class assessment is higher for operations conducted above 500 ft or 150 m (this is excluding additional air risk buffers) for most cases [1, p. 55]. A higher air risk class may require additional means to mitigate the risk of mid-air collisions. In contrast to the open category, no additional information is given on how to assess the HAG for operations in the specific category. In this work, the point on the ground directly below the drone is used as a reference to measure HAG for specific category operations. Also, an air risk buffer of ca. 100 ft is assumed resulting in an upper HAG limit of 120 m. Other, more specialized rules for specific category operations including Standard Scenarios, Predefined Risk Assessments (PDRAs), and rules related to flight nearby man-made obstacles are not considered in this work.

Fig. 1 illustrates the different HAG limits. It can be seen that the cylindrical constraint for manned aircraft leads to an vertical buffer between manned and unmanned traffic that increases with the slope of the terrain. Also, the point-wise vertical measurement as used for the specific category gives a more conservative upper limit than the distance measure from the closest terrain point as used for the open category.

3.2. DEM Availability and Accuracy

The proposed approach for HAG estimation depends on the availability of a DEM, more specifically a digital terrain model (DTM) as described in [11], with sufficient accuracy within the area of operation. In the following, we give an overview over available DEM products and their properties, most importantly their vertical accuracy. After discussing DEMs with global coverage, a focus is set on DEMs covering Germany due to the authors’ residency. An analysis of availability and accuracy of DEMs for other nations is beyond the scope of this work. Also, commercially available DEM products (e.g. [12]) are not considered in the following.

A set of global DEMs exist and are freely available that are based on data from the Shuttle Radar Topography Mission (SRTM) and Advanced Spaceborne Thermal Emission and Reflection Radiometer (ASTER) satellite missions [13] [14]. An overview and analysis of such DEMs can be found in [15, 16]. Also, the EU-DEM, which was created within the Copernicus program and covers the European Union, is mainly based on SRTM and ASTER data [17]. In [15]), an overview of global DEMs based on SRTM and ASTER data is given including a comparison of their accuracy. Although different error metrics are given, including root mean square error (RMSE), mean average error (MAE) and linear error with 90% confidence (LE90), which forbids a direct comparison, it can be seen that the overall vertical accuracy is in the range of 4-10 m. Considering an exemplary drone operation within VLL airspace, where the desired HAG range may be between 50 m and 120 m, this may not be sufficiently accurate, hence limiting the usefulness of SRTM- or ASTER-based DEMs for HAG estimation. However, as discussed in [18] for the EU-DEM the local terrain complexity has a significant impact on the accuracy. Therefore, for operations over mostly flat terrain, accuracy, and resolution of these DEMs may be sufficient. Public availability and a substantial number of validation studies are positive aspects to be mentioned.

Another DEM based on satellite data acquisition is the TanDEM-X DEM [19]. Compared to SRTM data which covers latitudes of roughly +/- 60° and ASTER data with coverage of +/- 83°, TanDEM-X has a global coverage including polar regions [20]. Its vertical accuracy is specified at 10 m with a 90 % linear error at a horizontal resolution of 0.4 arc seconds (which corresponds to 12 m at the equator). However, it has been shown that the vertical accuracy for moderate terrain is below 2 m absolute error.

For certain regions, DEMs based on LiDAR data are available with much higher accuracy than SRTM/ASTER-based DEMs. For example, the LiDAR Composite DTM 2022 is “a raster elevation

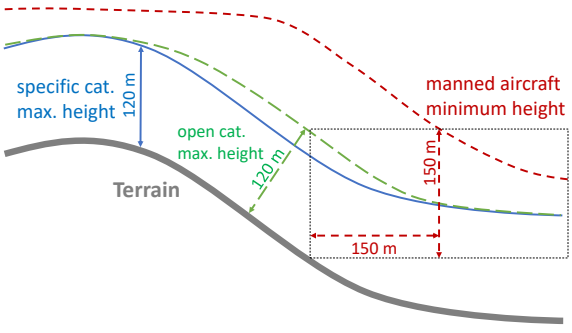

FIG 1. Illustration of different maximum/minimum HAG limits

model covering >95 % of England at 1m spatial resolution" with very recent data collected between 2020 and 2022 [21]. It is accessible publicly under an open data license. In Germany, LiDAR-based DEMs are accessible for all federal states individually. They are available under open data licenses for North-Rhine-Westphalia, Bavaria, Thuringia, Hessen, Saxony-Anhalt, Schleswig-Holstein, Berlin, Brandenburg, and Saxony. In contrast, Lower Saxony, Baden-Württemberg, Mecklenburg-Pomerania, Bremen, Saarland, Rhineland-Palatinate, and Hamburg offer them for a fee. Most of these LiDAR-based DEMs are regularly updated, e.g. Saxony-Anhalt performs annual airborne laser scanning and North-Rhine-Westphalia updates a fifth of its data each year. LiDAR-based DEMs usually feature a sub-meter vertical accuracy at high resolutions, e.g. the DEM provided by [22] is specified with a vertical accuracy of around 0.3 m RMSE, and in even terrains up to 0.15 m RMSE at 1 m horizontal resolution. As each federal state offers its own DEM product, data formats and map projections vary. For example, Saxony-Anhalt's DEM is provided as ASCII-based xyz-files where the data is given as a point list and coordinates are given in reference to UTM zone 32. In contrast, the Bavarian DEM is provided as GeoTIFF [23], the Saxony DEM uses UTM zone 33 coordinates.
Another factor to be considered with high resolution LiDAR-based DEMs is data storage requirements. For example, the DEM covering Bavaria provided by [23] would amount to 240 GB. For an onboard HAG estimation it would be advisable to tailor the elevation data to match the area of operation or - at the least - to stay below the storage capacity available. For example, the Pixhawk autopilot running the NuttX realtime operating is limited to memory cards storage capacity of 32 GB [24].

3.3. Qualitative Error Analysis

When estimating the HAG based solely on the current 3D position of a drone and a DEM, several error sources must be accounted for. With a thorough error analysis, a sensible upper bound of the total error E_{HAG} can be derived which must then be subtracted from the maximum HAG limit as an additional safety buffer in order to ensure compliance with the operational constraint of a maximum HAG. The vertical extent of the operational volume in typical VLL operations of only 120 m underlines the importance of approximating the maximum error as closely as possible to avoid unnecessarily conservative limitations. As calculating HAG essentially means to subtract the terrain elevation from the drone's altitude, the error may be decomposed into a navigation error $E_{HAG,NAV}$ and a terrain elevation error due to limited DEM accuracy $E_{HAG,DEM}$ such that

$$E_{HAG} = E_{HAG,NAV} + E_{HAG,DEM}. \tag{1}$$

These two main sources of errors are investigated in more detail in the following.

Navigation Error

For the HAG estimation, the earth-referenced position of the drone is used. For most drones, GNSS stands as the sole method for determining the absolute position. Hence, the accuracy of the GNSS navigation solution is considered the main factor in regard to the navigation error. Commercial off-the-shelf GNSS receivers, as commonly integrated in autopilot systems, are usually rated with an accuracy of several meters. Due to the fact that the position is obtained using trilateration of satellite positions, the reported altitude is usually less accurate than the horizontal position. In obstructed environments accuracy may decrease due to multi-path reception of the GNSS signal. However, for the use-case of estimating the HAG, this error source is assumed to be neglected as special rules apply when flying in close vicinity of obstacles. There are several technologies to increase accuracy of GNSS such as RTK, SBAS, or GBAS, however, these are not commonly integrated in drones as for most use-cases GNSS accuracy is sufficient.
The impact of the GNSS position error on the HAG estimation is twofold. Firstly, the vertical error $E_{NAV,z}$ directly influences the accuracy of the HAG estimate. Secondly, the horizontal error $E_{NAV,xy}$ can significantly impact the estimate in uneven terrain, as it may lead to incorrect terrain height lookup in the DEM. The impact of the horizontal error on the HAG estimate depends on the terrain slope Θ_T, such that the HAG error due to GNSS position errors accumulates to:

$$E_{HAG,NAV} = E_{NAV,z} + E_{NAV,xy} \sin \Theta_T \tag{2}$$

Terrain Elevation Error

As elaborated in 3.2, the accuracy of DEMs is often assessed in terms of statistical models derived from sampled validation points. Care must be taken when interpreting such statistical vertical accuracy metrics, e.g. RMSE. The vertical accuracy models incorporate a set of errors from different sources. A primary source of errors stems from the raw data measurement which have limited accuracy and resolution. Additionally, extracting terrain elevation from measurement points can be erroneous in regions with dense vegetation, man-made structures or complex terrain. Also, there are different approaches of validating DEMs that may affect the outcome of the accuracy assessment [11]. The expected error from a DEM's inherent limited accuracy is given by $E_{DEM,acc}$.
For uneven or rough terrain, horizontal and vertical accuracy of DEMs are systematically coupled as the terrain height is averaged over each grid cell. Assuming adequate interpolation techniques are used when evaluating the DEM, terrain features spanning multi-

ple grid cells can be well represented. It is worth noting, that using interpolation during the DEM validation process is common practice in order to minimize the impact of rasterisation on the accuracy model [11]. To estimate the remaining error from terrain features that are not well modelled due to the limited DEM resolution, several terrain properties, such as slope, roughness or curvature may be analyzed. In [25] for example, a conservative error estimate that varies locally based on these properties is added to a DEM to retrieve a conservative – in the sense of the addressed use-case – elevation estimate. In the context of the HAG estimation addressed in this work, we propose to model this error based on the horizontal resolution and the local terrain slope as "an indication of terrain complexity level" [26]. Given the horizontal resolution Δ_x, i.e. the edge length of each grid cell, the error may be modeled as a function $E_{DEM,res} = f(\Delta_x, \Theta_T)$.
Additional errors may arise due to the potential requirement for transforming the vertical datum and applying map projections in the HAG estimation process. Commonly, DEMs deliver an orthographic terrain height, i.e. the height above a reference geoid. In order to compare this height to an ellipsoidal height, as used by GNSS and consequently by common drone autopilot systems, the geoid height must be known. At first glance, this may appear to be a solvable or even trivial issue; however, vertical datums are a complex subject in the field of geodesy. Vertical reference systems are regularly updated to accommodate for changes like inter-continental drift. Also, not all vertical reference systems are publicly available. For example, the EU-DEM v1.1 uses the European Vertical Reference System EVRS2000 which has never been published [15, 17]. Potential errors that stem from vertical datum transformations or map projections are denoted as $E_{DEM,T/P}$.
Given these error sources, the total elevation error sums up to:

$$E_{HAG,DEM} = E_{DEM,acc} + E_{DEM,res}(\Delta_x, \Theta_T) + E_{DEM,T/P} \tag{3}$$

4. RUNTIME ASSURANCE ARCHITECTURE

When operating a drone within VLL airspaces, information about the HAG is crucial. Yet, the map-based HAG estimator is based on two main sources of uncertainty: GNSS altitude and position which is used to look up the local terrain elevation on one hand and the accuracy and availability of the DEM on the other hand. These uncertainties must be managed during flight before decisions are made based on HAG estimates.
To manage the uncertainties, we propose to integrate the HAG estimation into a runtime assurance architecture as described in [27,28]. As shown in Figure 2, the HAG estimation is integrated as one of many functions of the drone's *Autonomy Stack*. As it deals with untrusted information (GNSS, DEM elevation) and may involve complex functions (e.g. database look-ups) it is monitored by a *Safe Operation Monitor* (SOM) which checks both inputs and outputs of the HAG Estimator and may switch to a recovery function at any time such as alerting a safety pilot.
Regarding the assessment of untrusted function of the autonomy stack, the safe operation monitor is responsible to check the availability and validity of any external data source used by the function. In the case of the HAG estimation, this would include for example the number of GNSS satellites used to calculate the navigation solutions, any accuracy and validity information of the GNSS receiver itself, and the availability of the DEM at the current position. Also, input data could be validated using cross-checks between sensors, e.g. jumps in the GNSS position could be detected by comparison with INS sensor data. Furthermore, the outputs of untrusted functions are analysed by the monitor to see whether they are within valid bounds and consistent. For example, the expected HAG range for a specific mission could be limited to sensible values a priori to catch cases of faulty estimation leading to a large HAG discrepancy.

5. EXPERIMENTAL SETUP

In this section, we describe the setup of the experiment to validate the GNSS- and map-based HAG-Estimation approach. Also, we present the overall software and hardware architecture. Experimental results are presented in the next section.

5.1. Flight Test Demonstrator

For the experimental validation, a modified version of a DJI Matrice 600 Pro hexacopter was used that is depicted in Fig. 3. The copter was equipped with a Pixhawk autopilot that computes a navigation solution based on GNSS and INS sensor data. The navigation solution is then forwarded to a Nvidia Jetson companion computer that provides a ROS2 environment for software modules such as the HAG estimation and the Safe Operation Monitor. Further, a LiDAR sensor was integrated to provide a reference measurement to val-

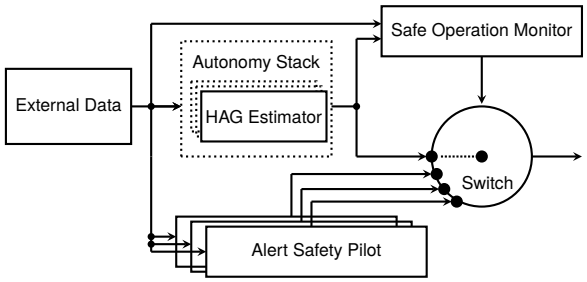

FIG 2. Simplified runtime assurance architecture for our DLR-Demonstrator. The HAG Estimator is part of the autonomy software stack, the Safe Operation Monitor checks validity of software stack and decides whether to activate a recovery function such as alerting a safety pilot.

FIG 3. DLR flight test demonstrator *CDO* equipped with GNSS and LiDAR sensors.

idate the estimated HAG. As the range of this sensor is limited to ca. 30 m, the flight altitude was limited by the range of the sensor. All flights were conducted at a height above the take-off point of roughly 20 m.

5.2. Software Considerations

The companion computer hosted two ROS2 nodes: the HAG Estimator and the Safe Operation Monitor. The HAG Estimator provides altitude information, while the Safe Operation Monitor first checks the validity of the HAG estimate and then uses the information to activate safety measures should operational limits be violated. We present the two ROS2 nodes next.

HAG Estimation

For our experiments, we used publicly available DEM based on LiDAR measurements with a horizontal resolution of 2 m available at [22]. The HAG Estimator uses information about the current position to look up the current terrain elevation in the DEM. The component is depicted in Fig. 4. First, the HAG estimator receives GNSS position information and transforms these into coordinates used by the DEM. Next, it queries the value of the DEM raster at these coordinates. No interpolation was used in our tests to simplify the experiment setup. For flights over uneven terrain, a linear interpolation may be used to increase the terrain elevation accuracy and provide a smooth HAG estimate in forward flight. After the terrain elevation query, the HAG estimate is calculated as the difference between the given GNSS altitude and the DEM terrain elevation. Finally, the HAG estimate is published.

Safe Operation Monitor

The task of the Safe Operation Monitor is to assess if the current flight is safe in regards to regulatory or operational constraints such as a maximum HAG. Therefore, the Safe Operation Monitor is one of the safety critical components of the aircraft. As such, it

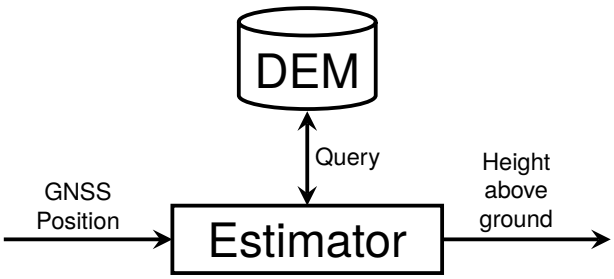

FIG 4. Data Flow Diagram of the map-based HAG Estimator.

needs to be implemented to strict safety standards. In our experimental setup, we used the formal specification language RTLola to capture properties that shall be monitored. An RTLola specification supports real-time language features [29], static analysis of the specification [30], and the automatic generation of executable monitors that provide guarantees for their correctness [31], for example. In general, RTLola strives for closing the gap between high-level natural language requirements and low-level executable code. An RTLola specification consists of *input* streams, *output* streams, and *triggers*. Input streams are data that are received by the monitor such as sensor readings. Output streams represent computations of the monitor. These computations can be either event-based, i.e. computations are executed whenever new inputs arrive, or periodic, i.e. each output has its own frequency at which it computes new values. Finally, triggers are notifications that some condition is satisfied.

```
input hag : Float32
const min_HAG : Float32 := 10.0
const max_HAG : Float32 := 20.0

output Δ_min := hag - min_HAG // violation if < 0
output Δ_max := max_HAG - hag // violation if < 0

output pctl_min @ 10Hz :=
  Δ_min.aggregate(over: 2s, using: pctl(95))
output pctl_max @ 10Hz :=
  Δ_max.aggregate(over: 2s, using: pctl(95))

trigger 0.0 ≤ pctl_min ≤ 1.0 "WARNING: lower bound"
trigger 0.0 ≤ pctl_max ≤ 1.0 "WARNING: upper bound"
trigger pctl_min < 0.0 "VIOLATION: lower bound"
trigger pctl_max < 0.0 "VIOLATION: upper bound"
```

Listing 1. An RTLola specification is given that checks if the received HAG is within its limits. The periodic outputs `pctl_min` and `pctl_max` compute the 95th percentile over a two-second window of the distances to the limits. This allows outliers to be filtered out and to take a robust decision on whether to activate a recovery function or not.

As an RTLola example consider Listing 1. The Listing shows how RTLola is used to check the outputs of the HAG Estimator as suggested in Section 4. Here, as single input, the HAG `hag` is received. Next, two constants are specified that represent the limits of `hag`. These limits are used by the outputs `Δ_min` and `Δ_max` to compute the distance of the current `hag` to its

FIG 5. Container cluster that is flown over during the mission.

limits. Note that a negative value indicates that a limit is violated. So far, the outputs are event-based, meaning they are evaluated each time a new value of `hag` arrives; the next outputs `pctl_min` and `pctl_max` are periodic and therefore have a specified frequency at which they are evaluated. The outputs `pctl_min` and `pctl_max` compute the 95th percentile of the Δ`_min` and Δ`_max`, respectively. Finally, there are four triggers, two of which represent warnings when the 95th percentile is close to being exceeded and the other two represent an exceedance of the limits.
How RTLola can be used to monitor the inputs of the HAG Estimator, we refer to [29]. In Figure 5 of this work, an RTLola specification that monitors GNSS sensor data is provided.

5.3. Mission

The flights were conducted at the DLR National Experimental Test Center for Unmanned Aircraft Systems[1], located at the airfield Magdeburg-Cochstedt. As typical for airfields, the operational area has a very flat terrain profile. After a manual take-off, a round-trip waypoint mission of approximately 160 m length was flown three times, at 15 m, 20 m, and 25 m above the take-off position. Finally, the drone landed at the initial take-off position. During each round trip mission, a container cluster on the apron was overflown that is depicted in Figure 5.

6. RESULTS

We separated the mission into three segments according to the different altitudes described in 5.3. The first segment depicted in Fig. 6a shows the take-off and the round trip flight at 15 meters altitude. The second segment depicted in Fig. 6b shows the round trip flight at 20 meters altitude. The third segment depicted in Fig. 6c shows the round trip flight at 25 meters altitude as well as the landing. In all figures, the target altitude is shown as dotted line as reference.

[1] https://www.dlr.de/en/dlr/locations-and-offices/cochstedt

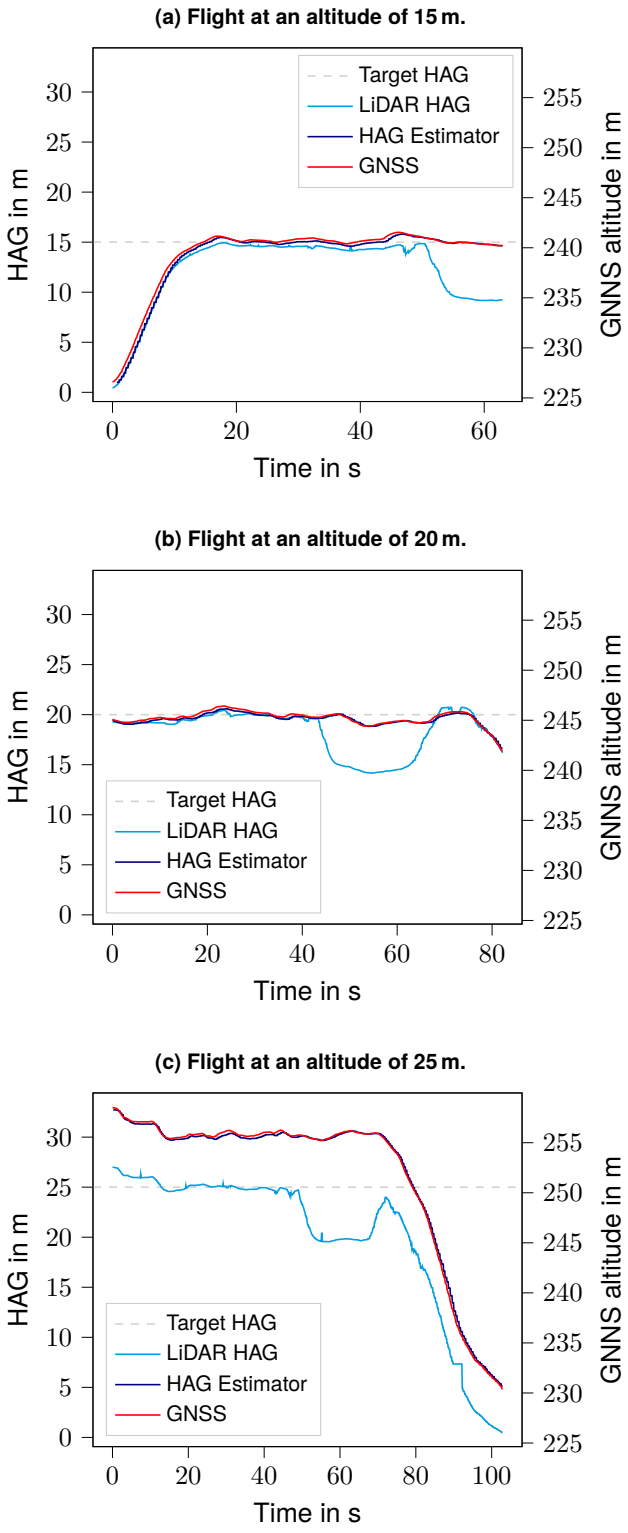

FIG 6. HAG data for flights at different altitudes. The plots show received data from the onboard GNSS, Sensor, LiDAR sensor, and map-based HAG estimator. The dashed line corresponds to the target HAG which has been specified in the waypoint mission.

Further, the LiDAR values, the GNSS altitude, and the unfiltered HAG estimation outcomes are depicted. The depicted LiDAR HAG is computed based on the smallest distance to a point in the range image of the LiDAR. This corresponds to the minimum distance to the ground, i.e. the current HAG. To account for noise in the LiDAR data as well as small objects on the ground, a block filter of size five is used to smooth the range image before calculating the minimal distance.

Observation 1 When overflying the container cluster, the HAG estimation stays approximately constant, however, the LiDAR HAG measurement changes in respect to the height the container cluster. This is expected behavior, as a digital terrain model should not account for man-made structures and the LiDAR measures against the surface of the container. This indicates that a map-based HAG estimation may actually be preferred over a direct sensor-based HAG measurement for the addressed use-case. When relying solely on distance measurements to the overflown surface, any man-made structures such as buildings will result in an underestimation of the HAG, hence, possibly leading to a violation of the maximum HAG which is in reference to the local terrain elevation. It should be noted that the DEM used here, although labelled as a digital terrain model, does show the footprints of permanent buildings. To avoid underestimating the HAG, a DTM that does not account for any man-made structures should be used.

Observation 2 Since the flights were performed over very flat terrain, the GNSS-based altitude above the take-off point coincides closely to the map-based HAG estimation. Hence, the common practice among drone pilots to monitor the HAG solely based on GNSS altitude is a valid approach for flight above flat terrain. The proposed map-based HAG estimation is targeted towards cases where the elevation difference of the overflown terrain is significant in respect to the maximum HAG limit.

Observation 3 In the first two flights, the LiDAR-based HAG estimation coincides closely with the map-based estimation. Only for the third flight, a constant bias between the two estimations can be observed. This offset can be largely attributed to the GNSS vertical accuracy, i.e. $E_{NAV,z}$. To analyze with confidence which other factors contribute to the error, more extensive experiments would have to be conducted.

7. CONCLUSIONS AND OUTLOOK

With increasing accuracy, resolution, and availability of DEMs, it becomes feasible to estimate the HAG onboard and in real-time solely relying on GNSS position information available as commonly available in autopilot systems. More specifically, the use of DEMs enables an accurate HAG estimation over uneven and complex terrain where the elevation of the take-off position cannot be used as a reference. Our assessment indicates that error margins in the range of 10 m may be feasible for operations over moderate, pre-dominantly flat terrain, given the use of high-accuracy LiDAR-based DEMs. This implies that VLL operations, commonly limited to 120 m HAG, could be safe-guarded based on the map-based HAG estimation. Experimental results from flight tests where the HAG estimation was validated against LiDAR measurements support this claim. With the integration into a system architecture that leverages runtime monitoring to safeguard the operation, we have given an example of how unassured system components can be safely integrated into drones to increase onboard capabilities.

In this work, we addressed a general HAG upper limit only. In future, for flight in the vicinity of man-made structures or obstacles, European regulations for drone operations provides a specific set of rules which extends the VLL airspace to be used by drones, e.g. as described for the EASA open category in [1, p.249f]. Given a database with obstacles, such as tall buildings, power-lines etc., the proposed approach could be extended to monitor these rules as well, i.e. to assess the vicinity to obstacles and the resulting specific HAG limit. Also, it could be assessed if the proposed runtime assurance architecture could be used to facilitate operations using the HAG range between 120 m and 150 m which imposes additional requirements as described in [1]. Regarding the experimental assessment, further flight tests in more challenging terrain should be performed to quantify and validate the error margins and to further demonstrate the feasibility of the proposed approach.

Contact address:

simon.schopferer@dlr.de

References

[1] Easy Access Rules for Unmanned Aircraft Systems (Regulations (EU) 2019/947 and 2019/945) - Revision from September 2022 - Available in pdf, xml, and online format. https://www.easa.europa.eu/en/document-library/easy-access-rules/easy-access-rules-unmanned-aircraft-systems-regulations-eu.

[2] Ross. Is your drone telling you the correct height to operate legally and safely? https://aviassist.com.au/drone-telling-correct-height-operate-legally-safely/, May 2017.

[3] Tracy Lennertz, Andrea Sparko, Kim Cardosi, Alan Yost, Andrew Kendra, Jason Lu, and Tom Sheridan. Pilots' Estimation of Altitude of a Small Unmanned Aircraft System (sUAS). *Proceedings of the Human Factors and Ergonomics Society Annual Meeting*, 62:49–53, Sept. 2018. DOI: 10.1177/1541931218621011.

[4] Daniel Unger, I.-Kuai Hung, David Kulhavy, Yanli Zhang, and Kai Busch-Petersen. Accuracy of Unmanned Aerial System (Drone) Height Measurements. *International Journal of Geospatial*

and Environmental Research, 5(1), Jan. 2018. ISSN: 2332-2047.

[5] Markus Schartel, Ralf Burr, Pirmin Schoeder, Gilberto Rossi, Philipp Hugler, Winfried Mayer, and Christian Waldschmidt. Radar-based altitude over ground estimation of UAVs. In *2018 11th German Microwave Conference (GeMiC)*, pages 103–106, Freiburg, Germany, Mar. 2018. IEEE. ISBN: 978-3-9812668-8-7. DOI: 10.23919/GEMIC.2018.8335039.

[6] Igor S. G. Campos, Erickson R. Nascimento, Gustavo M. Freitas, and Luiz Chaimowicz. A Height Estimation Approach for Terrain Following Flights from Monocular Vision. *Sensors (Basel, Switzerland)*, 16(12):2071, Dec. 2016. ISSN: 1424-8220. DOI: 10.3390/s16122071.

[7] Anoop Cherian, Jon Andersh, Vassilios Morellas, Nikolaos Papanikolopoulos, and Bernard Mettler. Autonomous altitude estimation of a UAV using a single onboard camera. In *2009 IEEE/RSJ International Conference on Intelligent Robots and Systems*, pages 3900–3905, St. Louis, MO, USA, Oct. 2009. IEEE. ISBN: 978-1-4244-3803-7. DOI: 10.1109/IROS.2009.5354307.

[8] Cary R. Spitzer, editor. *Digital Avionics Handbook: Elements, Software, and Functions. Avionics*. Electrical Engineering Handbook Series. CRC Press, Boca Raton, 2nd ed edition, 2007. ISBN: 978-0-8493-8438-7.

[9] Paul Sorokowski, Mark Skoog, Scott Burrows, and SaraKatie Thomas. Small UAV Automatic Ground Collision Avoidance System Design Considerations and Flight Test Results. Technical Report NASA/TM-2015-218732, June 2015.

[10] Easy Access Rules for Standardised European Rules of the Air (SERA) - Revision from February 2023 – Available in pdf, online & XML format. https://www.easa.europa.eu/en/document-library/easy-access-rules/easy-access-rules-standardised-european-rules-air-sera.

[11] José L. Mesa-Mingorance and Francisco J. Ariza-López. Accuracy Assessment of Digital Elevation Models (DEMs): A Critical Review of Practices of the Past Three Decades. *Remote Sensing*, 12(16):2630, Jan. 2020. ISSN: 2072-4292. DOI: 10.3390/rs12162630.

[12] Lido Surface Data NEXTView (Terrain). https://www.lhsystems.com/solutions/flight-operations-solutions/lido-data-solutions/lido-surface-data/lido-surface-data-0, Feb. 2020.

[13] Tom G. Farr, Paul A. Rosen, Edward Caro, Robert Crippen, Riley Duren, Scott Hensley, Michael Kobrick, Mimi Paller, Ernesto Rodriguez, Ladislav Roth, David Seal, Scott Shaffer, Joanne Shimada, Jeffrey Umland, Marian Werner, Michael Oskin, Douglas Burbank, and Douglas Alsdorf. The Shuttle Radar Topography Mission. *Reviews of Geophysics*, 45(2):RG2004, May 2007. ISSN: 8755-1209. DOI: 10.1029/2005RG000183.

[14] Michael Abrams, Hiroji Tsu, Glynn Hulley, Koki Iwao, David Pieri, Tom Cudahy, and Jeffrey Kargel. The Advanced Spaceborne Thermal Emission and Reflection Radiometer (ASTER) after fifteen years: Review of global products. *International Journal of Applied Earth Observation and Geoinformation*, 38:292–301, June 2015. ISSN: 15698432. DOI: 10.1016/j.jag.2015.01.013.

[15] Ricardo Tavares da Costa, Paolo Mazzoli, and Stefano Bagli. Limitations Posed by Free DEMs in Watershed Studies: The Case of River Tanaro in Italy. *Frontiers in Earth Science*, 7, 2019. ISSN: 2296-6463.

[16] Guy J-P. Schumann and Paul D. Bates. The Need for a High-Accuracy, Open-Access Global DEM. *Frontiers in Earth Science*, 6, 2018. ISSN: 2296-6463.

[17] EU-DEM v1.1 — Copernicus Land Monitoring Service. https://land.copernicus.eu/imagery-in-situ/eu-dem/eu-dem-v1.1.

[18] EU-DEM - Report on the Results of the Statistical Validation — Copernicus Land Monitoring Service. https://land.copernicus.eu/user-corner/technical-library/eu-dem-2013-report-on-the-results-of-the-statistical-validation.

[19] TanDEM-X Science Server. https://tandemx-science.dlr.de/.

[20] Christopher Wecklich, Carolina Gonzalez, and Paola Rizzoli. TANDEM-X height performance and data coverage. In *2017 IEEE International Geoscience and Remote Sensing Symposium (IGARSS)*, pages 4088–4091, Fort Worth, TX, July 2017. IEEE. ISBN: 978-1-5090-4951-6. DOI: 10.1109/IGARSS.2017.8127898.

[21] Defra Data Services Platform. https://environment.data.gov.uk/dataset/13787b9a-26a4-4775-8523-806d13af58fc.

[22] Sachsen Anhalt DGM - Digitales Geländemodell. https://www.lvermgeo.sachsen-anhalt.de/de/gdp-dgm-dom-lsa.html.

[23] Bayerische Vermessungsverwaltung - Digitales Geländemodell 1m (DGM1). https://geodaten.bayern.de/opengeodata/OpenDataDetail.html?pn=dgm1.

[24] Logging | PX4 User Guide. https://docs.px4.io/main/en/dev_log/logging.html.

[25] J. Schiefele, M. Launer, C. Pschierer, D. Howland, B. Dorrell, and M. Fox. A worldwide SRTM terrain database suitable for aviation use. In *Enhanced and Synthetic Vision 2006*, volume 6226, pages 27–36. SPIE, May 2006. DOI: 10.1117/12.664898.

[26] Thierry Toutin. Impact of terrain slope and aspect on radargrammetric DEM accuracy. *ISPRS Journal of Photogrammetry and Remote Sensing*, 57(3):228–240, Dec. 2002. ISSN: 0924-2716. DOI: 10.1016/S0924-2716(02)00123-5.

[27] D. Seto, B. Krogh, L. Sha, and A. Chutinan. The simplex architecture for safe online control system upgrades. In *Proceedings of the 1998 American Control Conference. ACC (IEEE Cat. No.98CH36207)*, volume 6, pages 3504–3508 vol.6, 1998. DOI: 10.1109/ACC.1998.703255.

[28] Pranav Nagarajan, Suresh K Kannan, Christoph Torens, Mike E Vukas, and George F Wilber. ASTM F3269 - an industry standard on run time assurance for aircraft systems. In *AIAA Scitech 2021 Forum*, page 0525, 2021.

[29] Jan Baumeister, Bernd Finkbeiner, Sebastian Schirmer, Maximilian Schwenger, and Christoph Torens. RTLola cleared for take-off: monitoring autonomous aircraft. In *Computer Aided Verification: 32nd International Conference, CAV 2020, Los Angeles, CA, USA, July 21–24, 2020, Proceedings, Part II 32*, pages 28–39. Springer, 2020.

[30] Johann C Dauer, Bernd Finkbeiner, and Sebastian Schirmer. Monitoring with verified guarantees. In *International Conference on Runtime Verification*, pages 62–80. Springer, 2021.

[31] Bernd Finkbeiner, Stefan Oswald, Noemi Passing, and Maximilian Schwenger. Verified rust monitors for lola specifications. In *International Conference on Runtime Verification*, pages 431–450. Springer, 2020.